Problems of Robustness in Poisson−Boltzmann Binding Free Energies

Robert C. Harris,[†] Travis Mackoy,[‡] and Marcia O. Fenley*[,¶]

[†]Sealy Center for Structural Biology and Molecular Biophysics, University of Texas Medical Branch, 301 University Boulevard, Galveston, Texas 77555-0304, United States

[‡]Department of Chemistry and Biochemistry, Duquesne University, Pittsburgh, Pennsylvania 15282, United States, and

[¶]Institute of Molecular Biophysics, Florida State University, Tallahassee, Florida 32306, United States

ABSTRACT: Although models based on the Poisson−Boltzmann (PB) equation have been fairly successful at predicting some experimental quantities, such as solvation free energies (ΔG), these models have not been consistently successful at predicting binding free energies ($\Delta\Delta G$). Here we found that ranking a set of protein−protein complexes by the electrostatic component ($\Delta\Delta G_{el}$) of $\Delta\Delta G$ was more difficult than ranking the same molecules by the electrostatic component (ΔG_{el}) of ΔG. This finding was unexpected because $\Delta\Delta G_{el}$ can be calculated by combining estimates of ΔG_{el} for the complex and its components with estimates of the $\Delta\Delta G_{el}$ in vacuum. One might therefore expect that if a theory gave reliable estimates of ΔG_{el}, then its estimates of $\Delta\Delta G_{el}$ would be reliable. However, $\Delta\Delta G_{el}$ for these complexes were orders of magnitude smaller than ΔG_{el}, so although estimates of ΔG_{el} obtained with different force fields and surface definitions were highly correlated, similar estimates of $\Delta\Delta G_{el}$ were often not correlated.

VDW   SE

INTRODUCTION

Classical molecular dynamics (MD) methods[1,2] have been fairly successful at predicting a wide variety of biophysical quantities, including solvation free energies (ΔG),[3−5] but computing binding free energies ($\Delta\Delta G$) with such methods is computationally expensive. Implicit solvent models, such as the Poisson−Boltzmann (PB) equation (PBE),[6−10] that average over the degrees of freedom of the solvent have therefore been developed to predict these quantities more quickly. The basic strategy of PB methods is to model the effects of the solvating waters by treating the molecule as a set of point charges in a low-dielectric region with a surrounding high-dielectric medium and to replace the surrounding ions with a continuous charge distribution outside the molecule that changes self-consistently in response to the electric field generated by the fixed charges in the molecule. These models have been fairly successful at predicting many biophysical quantities, including ΔG of small molecules[3,5,11−15] and the salt dependences of $\Delta\Delta G$.[16−22]

If estimates of $\Delta\Delta G$ could be obtained quickly from implicit solvent models, drug development and discovery could be accelerated. However, although implicit solvent models, including PB methods, have been successful at predicting ΔG,[3,5,11−15] they have been less successful at predicting $\Delta\Delta G$.[23−30] At first glance, this statement appears to be self-contradictory because the electrostatic component ($\Delta\Delta G_{el}$) of $\Delta\Delta G$ can be computed from

$$\Delta\Delta G_{el} = \Delta G_{el}^{comp} - \Delta G_{el}^1 - \Delta G_{el}^2 + \Delta\Delta G_{el}^C \qquad (1)$$

where ΔG_{el}^{comp} is the electrostatic component (ΔG_{el}) of ΔG of the complex, ΔG_{el}^1 and ΔG_{el}^2 are the ΔG_{el} of the two components of the complex, and $\Delta\Delta G_{el}^C$ is the electrostatic binding free energy

of the complex in vacuum. One might therefore initially think that if implicit solvent models can accurately rank molecules by ΔG, then they should be able to similarly rank complexes by $\Delta\Delta G$, but, as shown in the Results, this assumption is not necessarily true.

One potential explanation of this apparent contradiction is explored in the present work. In this study, ΔG_{el} was orders of magnitude larger than $\Delta\Delta G_{el}$. Therefore, estimates of ΔG_{el} with small relative errors combined to yield estimates of $\Delta\Delta G_{el}$ that contained large relative errors. All of the methods examined led to estimates of ΔG_{el} that were highly correlated with each other, but the individual estimates of ΔG_{el} could differ by hundreds of kJ/mol. These differences did not affect the rankings of these molecules by ΔG_{el} because ΔG_{el} covered a range of tens of thousands of kJ/mol, but the rankings by $\Delta\Delta G_{el}$ were affected because $\Delta\Delta G_{el}$ only covered a range of hundreds of kJ/mol.

One possible source of these errors is uncertainty in the force field used to specify the atomic charges and radii. These parameters were taken from the AMBER 94[31] and CHARMM 27[32] force fields, which were both created for classical MD simulations. Partly because these force fields were not designed specifically for implicit solvent models, using them could introduce errors into the calculations.[33−35] The choice of force field led to large absolute changes in ΔG_{el} (ranging from 39−2640 kJ/mol), but these changes did not lead to significant changes in the rankings of the molecules by ΔG_{el} because of the large range of ΔG_{el}. The rankings of complexes by $\Delta\Delta G_{el}$ were
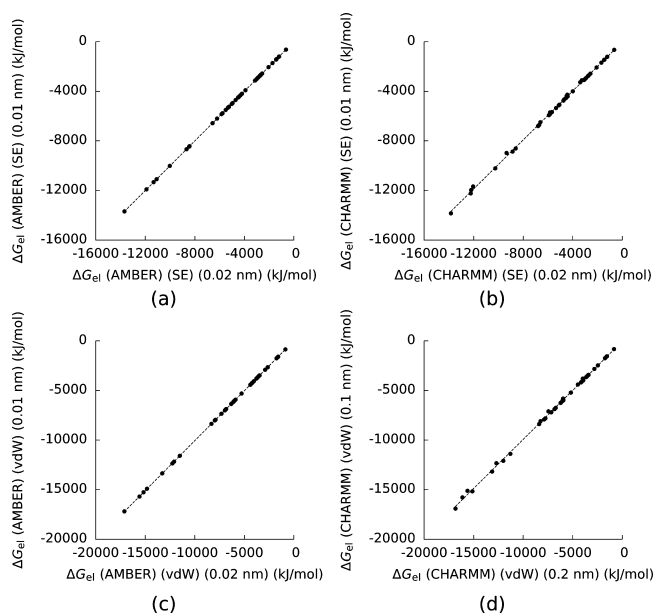
Figure 1. a) The electrostatic solvation free energy (ΔG_{el}) for the complexes and their components computed with the AMBER force field, the solvent-excluded (SE) surface, and a mesh spacing of 0.01 nm plotted against the same numbers computed with a mesh spacing of 0.02 nm. b), c), and d) are the same figures using the CHARMM force field and the SE surface, the AMBER force field and the van der Waals (vdW) surface, and the CHARMM force field and the vdW surface. The dotted lines are least-squares fits to the data. For a) the square of the Pearson correlation coefficient (R^2) is 0.99999996, for b) $R^2 = 0.9993$, for c) $R^2 = 0.999997$, and for d) $R^2 = 0.9991$.
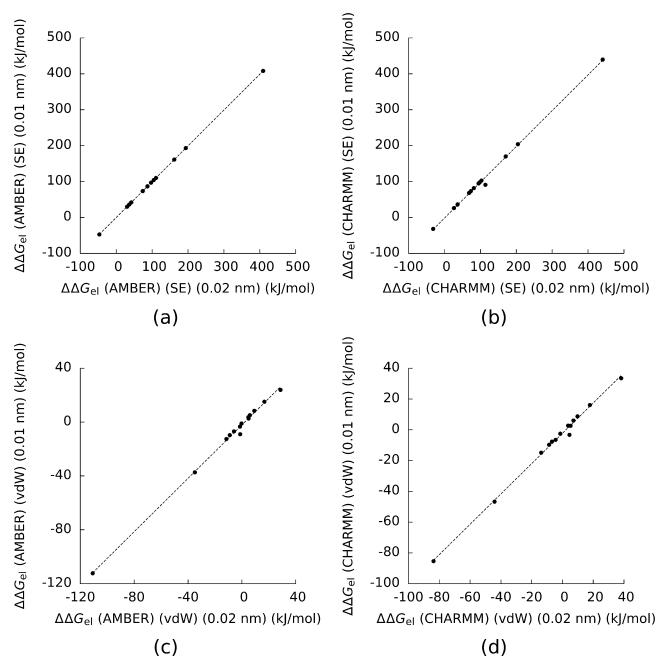

Figure 2. a) The electrostatic binding free energy ($\Delta\Delta G_{el}$) for the complexes and their components computed with the AMBER force field, the solvent-excluded (SE) surface, and a mesh spacing of 0.01 nm plotted against the same numbers computed with a mesh spacing of 0.02 nm. b), c), and d) are the same figures using the CHARMM force field and the SE surface, the AMBER force field and the van der Waals (vdW) surface, and the CHARMM force field and the vdW surface. The dotted lines are least-squares fits to the data. For a) the square of the Pearson correlation coefficient (R^2) is 0.999997, for b) $R^2 = 0.997$, for c) $R^2 = 0.997$, and for d) $R^2 = 0.996$.

also not strongly affected by the choice of force field, but the large absolute errors in these free energies (ranging from 0.3−112 kJ/mol) could cause problems for applications, such as drug development, where complexes may differ in $\Delta\Delta G_{el}$ on the order of 1 kJ/mol.

Another potential source of error is the method chosen to define the boundary between the molecular interior and exterior. Several surface definitions have been used in implicit solvent models. The most common choice is the solvent-excluded (SE) surface,[36,37] but other surfaces are advocated by some researchers, including the van der Waals (vdW) surface,[38−40] Gaussian surfaces,[41,42] and self-consistent surfaces.[43−47] No consensus has yet emerged about which of these surfaces is most realistic or best matches experimental data. For the complexes in the present study, although the SE surface produced predictions of ΔG_{el} that were highly correlated with those given by the vdW surface, the predictions of $\Delta\Delta G_{el}$ by these two surfaces were not strongly correlated. To further explore the uncertainties in these free energies generated by the uncertainties in the surface definition, we used a modified version of the vdW surface[48] (mvdW) to examine how these free energies changed as the definition of the surface was gradually changed. As the gaps and crevices inside the vdW surface were filled in as the radius of the probe used to define the mvdW surface was increased, ΔG_{el} increased smoothly and monotonically. These increases in ΔG_{el} probably reflected the losses of the favorable interactions between these regions of high dielectric constant and the nearby charges. However, the dependence of $\Delta\Delta G_{el}$ on probe radius was less predictable and nonmonotonic. Because ΔG_{el} changed smoothly and monotonically with probe radius, the rankings of these complexes by ΔG_{el} were not strongly sensitive to the choice

of probe radius, but the complicated dependences of the $\Delta\Delta G_{el}$ on probe radius made the rankings by $\Delta\Delta G_{el}$ sensitive to the choice of probe radius.

If the results presented here are transferable to other molecular complexes, they could help explain why PB models have been less successful at ranking complexes by $\Delta\Delta G$ than at ranking them by ΔG. Perhaps the predictions of $\Delta\Delta G$ by PB methods could be improved by obtaining better force fields and by determining what surface definition best matches experimental data. However, trying to do so by comparing the predictions of ΔG given by PB methods to experimental measurements may be difficult. In addition to ΔG_{el} and $\Delta\Delta G_{el}$, ΔG and $\Delta\Delta G$ contain nonelectrostatic components that are also somewhat uncertain.[49−52] Therefore, most of these comparisons are performed by determining whether the predictions of the PB methods are correlated with the experimental measurements, not by comparing the absolute values of these free energies. Because the uncertainties in the force field and molecular surface definition did not significantly change the rankings of these complexes by ΔG_{el} but did change the rankings by $\Delta\Delta G_{el}$, such experimental data would not have provided enough information to improve the predictions of $\Delta\Delta G_{el}$. Attempting to improve the predictions of ΔG given by PB models may not provide enough information to improve their predictions of $\Delta\Delta G$.

■ METHODS

We chose 14 complexes from the RCSB Protein Data Bank[53] by searching for high-resolution X-ray structures of protein−protein complexes where the components of the complex had a wide variety of interfacial shapes and charges. The pdbids and chains
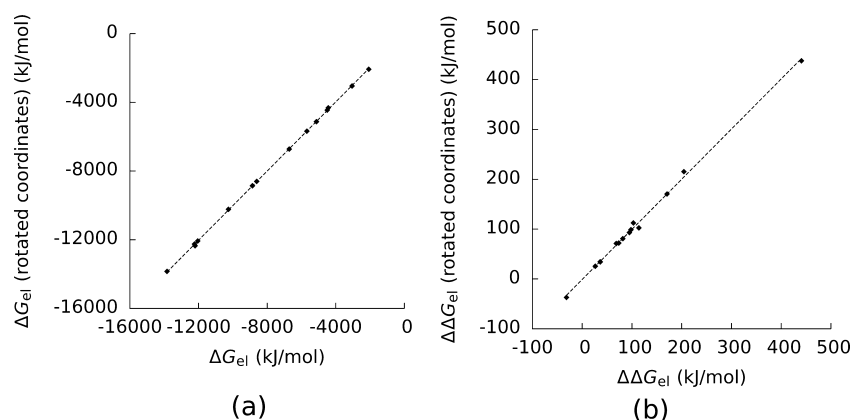
(a) (b)

Figure 3. a) The electrostatic solvation energy (ΔG_{el}) for the complexes and their components computed with the CHARMM force field, the solvent-excluded surface, and coordinates rotated around the x-axis by 45 deg plotted against the same values computed with nonrotated coordinates. b) The same plot for the electrostatic binding free energy ($\Delta\Delta G_{el}$. For a) the square of the Pearson correlation coefficient (R^2) was equal to 0.99992, and the square of the Spearman correlation coefficient (R_S^2) was equal to 0.996. For b) $R^2 = 0.999$, and $R_S^2 = 0.996$.

used as the binding components were as follows: 1acb chains E and I, 1atn chains A and D, 1avx chains A and B, 1b6c chains A and B, 1beb chains A and B, 1brs chains A and D, 1buh chains A and B, 1h1v chains A and G, 1he8 chains A and B, 1kxp chains A and D, 1sbb chains A and B, 1ysl chains A and B, 2hp0 chains A and B, and 2uy1 chains A and B. The coordinates of the protein atoms in these chains were taken from the structure files. The atomic partial charges were taken from the CHARMM 27[32] and AMBER 94[31] force fields. The radii were taken to be half the distance to the Lennard-Jones potential energy minimum between two atoms of the type in question. These charges and radii were added to the structures with the pdb2pqr utility.[54,55] All protein residues were assumed to be in their standard ionization states at pH = 7. All PB calculations were performed with the Cartesian PB (CPB) solver.[56] The locations of the atoms were fixed at the coordinates given in the structure files. No attempt was made to model conformational changes. All of these calculations used an interior dielectric constant of 1, an exterior dielectric constant of 80, a temperature of 298.15 K, a 1:1 salt concentration of 0.1 M, a grid that extended 2 times the largest dimensions of the complex, a finest grid spacing of 0.02 nm, and charge-conserving boundary conditions.[57]

The vdW surface defines the interior of the molecule to be the interiors of the set of spheres centered at the charge sites with radii equal to the vdW radii in the force fields. The SE surface defines the exterior of the molecule as the regions that can be contained within a probe sphere that does not overlap any of the vdW spheres. We used a probe radius of 0.14 nm to define the SE surface. The mvdW surface[48] is similar to the vdW surface, but any spheres that would not have solvent-accessible surface area in a SE surface with a given probe radius have their vdW radii increased by the probe radius. The internal crevices present in the vdW surface are therefore filled in as the probe radius used to define the mvdW surface is increased.

■ RESULTS

Convergence with Respect to Grid Spacing. Ensuring that PB results are converged is necessary in any PB application.[58,59] To this end, we recomputed ΔG_{el} and $\Delta\Delta G_{el}$ with both the AMBER and CHARMM force fields and with both the SE and vdW surfaces with a mesh spacing of 0.01 nm and compared the results to those obtained with a mesh spacing of 0.02 nm (Figure 1 and Figure 2). The results obtained at 0.01 nm were in
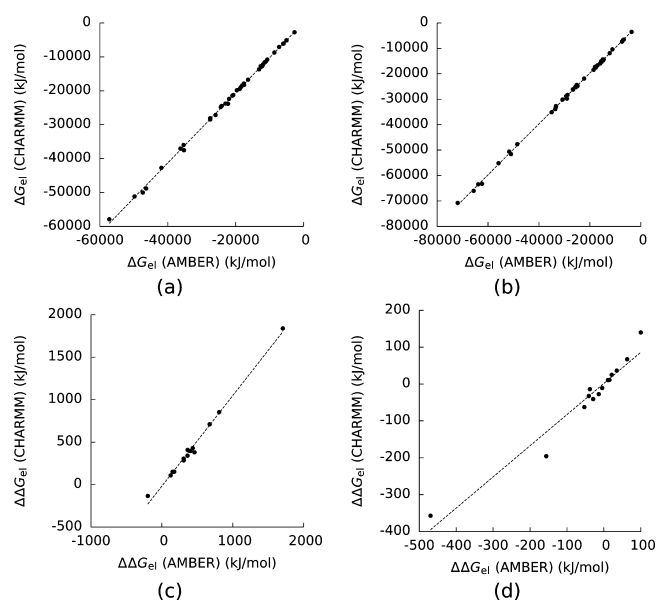

(a) (b)

(c) (d)

Figure 4. Electrostatic solvation free energies (ΔG_{el}) for the complexes and their components computed with the CHARMM force field plotted against those with the AMBER force field created with (a) a solvent-excluded surface and (b) a van der Waals surface. (c) and (d) show the same plots for the electrostatic binding free energies ($\Delta\Delta G_{el}$). For (a) and (b) the Pearson correlation coefficient (R^2) of the least-squares line was greater than 0.99999, and the Spearman correlation coefficients (R_S^2) were 0.998 and 0.998. For (c) and (d) $R^2 = 0.99$ and 0.95, and $R_S^2 = 0.965$ and 0.978. The dashed lines are least-squares lines drawn through the data.

good agreement with those we obtained with a grid spacing of 0.02 nm. For the remainder of the paper, we will only consider results obtained with a grid spacing of 0.02 nm.

To further test that our results had reached convergence, we recomputed ΔG_{el} and $\Delta\Delta G_{el}$ with a grid spacing of 0.02 nm, the CHARMM force field, and the SE surface after rotating the coordinates of the molecules around the x-axis by 45 deg. Figure 3 shows that these new values were highly correlated with our original data. (The square of the Pearson correlation coefficient (R^2) was 0.99992 for ΔG_{el} and $R^2 = 0.999$ for $\Delta\Delta G_{el}$.) We can therefore conclude that for those plots where $R^2 \ll 1$ this lack of correlation was not caused by numerical errors.

Force Field Choice. The choice of force field did not strongly affect the ordering of the molecules by ΔG_{el} (Figure 4),
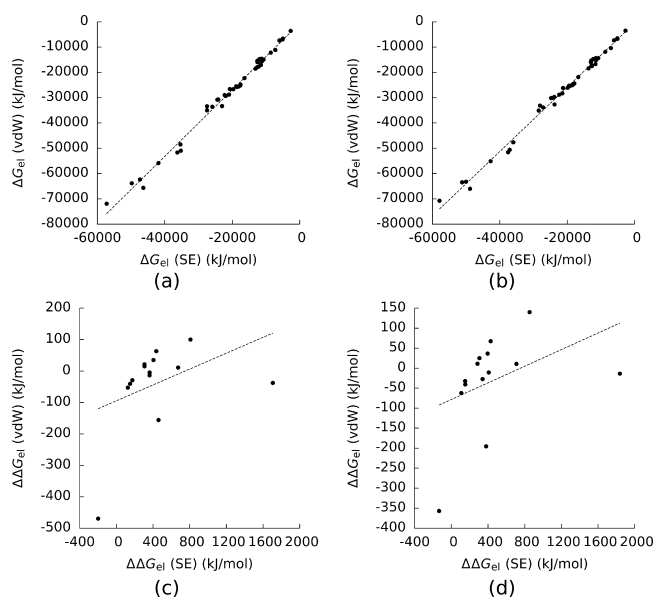
Figure 5. Electrostatic solvation free energies (ΔG_{el}) for the complexes and their components computed with the van der Waals (vdW) surface plotted against those with the solvent-excluded (SE) surface created with (a) the AMBER force field and (b) the CHARMM force field. (c) and (d) show the same plots for the electrostatic binding free energies ($\Delta\Delta G_{el}$). For (a) and (b) the Pearson and Spearman correlation coefficients (R^2 and R_S^2) of the least-squares line were greater than 0.99. For (c) and (d) $R^2 = 0.16$ and 0.17, and $R_S^2 = 0.45$ and 0.63. The dashed lines are least-squares lines drawn through the data.

as the Spearman correlation coefficients (R_S^2) were large. The R^2 between the ΔG_{el} computed with the AMBER force field and those computed with the CHARMM force field was greater than 0.99999 when either the vdW or SE surface was used. However, these R^2 were this large partly because ΔG_{el} covered a relatively large range, and simply using these correlation coefficients to judge the accuracy of this method would obscure some large uncertainties for individual molecules. The individual ΔG_{el} given by the AMBER force field differed from those given by the CHARMM force field by between 39 and 2640 kJ/mol when the SE surface was used and 8 and 1180 kJ/mol when the vdW surface was used. These estimates were still accurate enough to generate large R^2 because the ΔG_{el} of these molecules covered a range of more than 50000 kJ/mol.

The rankings of the complexes by $\Delta\Delta G_{el}$, like the rankings of the molecules by ΔG_{el}, were not strongly sensitive to the choice of force field, as a plot of the results given by the CHARMM force field versus those given by the AMBER force field had $R^2 = 0.99$ and $R_S^2 = 0.965$ when the SE surface was used and $R^2 = 0.95$ and $R_S^2 = 0.978$ when the vdW surface was used (Figure 4). However, the differences between the predictions given by the two force fields ranged from 0.15–127 kJ/mol when the SE surface was used and from 0.3–112 kJ/mol when the vdW surface was used.

Surface Definition. Figure 5 shows the ΔG_{el} computed with the SE surface plotted against those computed with the vdW surface for both the AMBER and CHARMM force fields. For both force fields, the vdW surface predicted consistently larger magnitudes of ΔG_{el}. The slopes of the least-squares lines in the first two plots in Figure 5 were 0.75 and 0.78, but this difference did not affect the ranking of the complexes by ΔG_{el}. (For both of these plots $R^2 > 0.99$ and $R_S^2 > 0.99$.)

In contrast, the rankings of these complexes by $\Delta\Delta G_{el}$ (Figure 5) were very sensitive to the choice of surface definition.
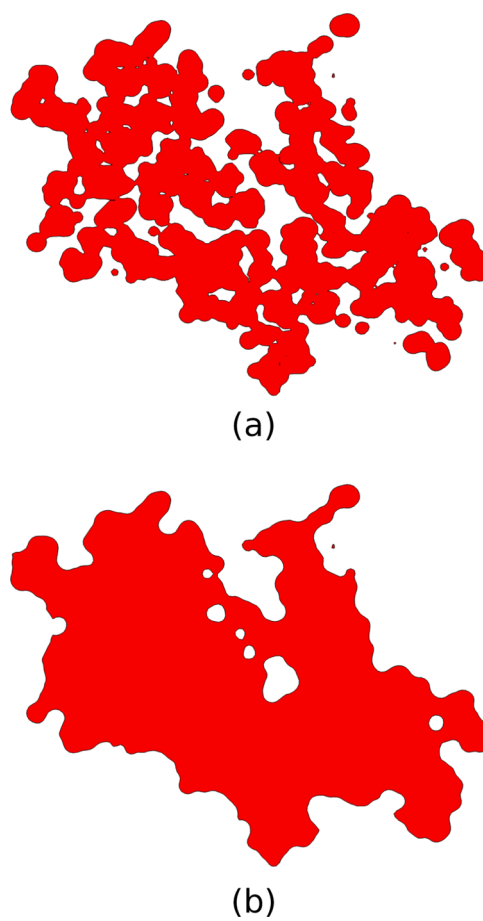

Figure 6. Slices through chain A of the 1he8 complex. The contours trace the boundary between the molecular interior and exterior for a) the van der Waals and b) the solvent-excluded surfaces.

($R^2 = 0.16$ and 0.17 and $R_S^2 = 0.45$ and 0.63.) The predictions of $\Delta\Delta G_{el}$ given by the two surface definitions differed by between 177 and 1745 kJ/mol.

Gradually Varying the Surface Definition. As shown in the previous section, the estimates of $\Delta\Delta G_{el}$ given by the SE surface differed substantially from those given by the vdW surface. Although both the SE and vdW surfaces agree that the region contained within the vdW radii of the solute atoms should be treated as interior to the solute, the charges in the vdW surface are more solvent exposed than those in the SE surface because the vdW surface contains gaps and crevices of high dielectric inside the molecule, whereas the SE surface does not (Figure 6).

Whether these crevices should be considered to be solvated is still an active area of research,[38−40] and we wanted to know how the PBE's predictions of ΔG_{el} and $\Delta\Delta G_{el}$ changed as these crevices were gradually filled. To this end, we considered the mvdW surface. The mvdW surface was originally designed to mimic the SE surface when the probe radius was set to 1.4 Å,[48] and its predictions of ΔG_{el} were indeed highly correlated with those of the SE surface (Figure 7). ($R^2 = 0.98$ for the AMBER force field and 0.99 for CHARMM.) However, its predictions of $\Delta\Delta G_{el}$ were not. ($R^2 = 0.13$ for the AMBER force field and 0.30 for CHARMM.) Once again, that a surface definition produced estimates of ΔG_{el} that were highly correlated with those given by the SE surface did not guarantee that its predictions of $\Delta\Delta G_{el}$ would be similarly highly correlated with those of the SE surface.
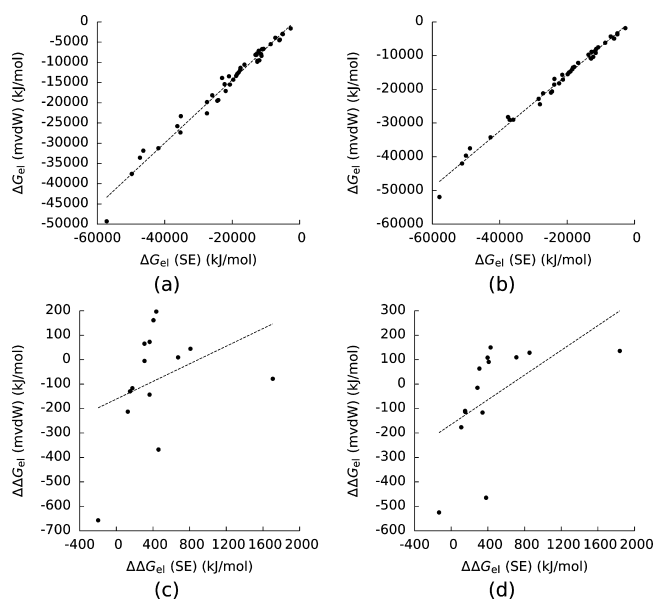
Figure 7. Electrostatic solvation free energies (ΔG_{el}) for the complexes and their components computed with the modified van der Waals (mvdW) surface plotted against those with the solvent-excluded (SE) surface created with (a) the AMBER force field and (b) the CHARMM force field. (c) and (d) show the same plots for the electrostatic binding free energies ($\Delta\Delta G_{el}$). For (a) and (b) the Pearson correlation coefficients (R^2) of the least-squares lines were 0.98 and 0.99. For (c) and (d) $R^2 = 0.13$ and 0.30. The dashed lines are least-squares lines drawn through the data.

In Table 1, the ΔG_{el} of the complexes and the $\Delta\Delta G_{el}$ are shown as functions of the probe radius in the mvdW surface. Possibly because the charges in the molecules were less solvent exposed as the probe radius was increased, ΔG_{el} increased monotonically with probe radius. A typical example is shown in Figure 8, where ΔG_{el} for the complex with the pdbid 1kxp is shown as a function of probe radius. However, the dependence of $\Delta\Delta G_{el}$ on probe radius is more complex. In Figure 8 $\Delta\Delta G_{el}$ for 1kxp is displayed, and unlike ΔG_{el} for this complex, $\Delta\Delta G_{el}$ did not vary monotonically with probe radius. Although $\Delta\Delta G_{el}^C$ did not depend on probe radius and the ΔG_{el} all increased monotonically with surface area, $\Delta\Delta G_{el} = \Delta G_{comp} - \Delta G_1 - \Delta G_2 + \Delta\Delta G_{el}^C$ had no simple dependence on probe radius and was instead a complicated function of the molecular shape and charge distribution.

CONCLUSIONS

Implicit solvent methods based on the PBE[6−10] have been fairly successful at predicting a wide range of biophysical quantities, including ΔG[3,5,11−15] and the salt dependence of $\Delta\Delta G$.[16−22] Because these methods eliminate the need to consider the degrees of freedom of the solvent by integrating over them, they are a fast alternative to methods, such as MD methods,[1,2] that explicitly account for those degrees of freedom. In particular, if PB methods could be used to obtain fast and accurate estimates of $\Delta\Delta G$, they could complement slow, expensive experimental screening of compound libraries in drug-development studies,

Table 1. Electrostatic Solvation (ΔG_{el}) and Binding ($\Delta\Delta G_{el}$) Free Energies for the Complexes in This Study Computed with the Modified van der Waals Surface and the AMBER Force Field As Functions of Probe Radius[a]

complexes		probe radii (nm)							
		0.01	0.02	0.04	0.06	0.08	0.1	0.12	0.14
1acb	ΔG_{el}	−16941	−16107	−14482	−12847	−11387	−9987	−8781	−7810
	$\Delta\Delta G_{el}$	−39	−37	−39	−30	−41	−70	−102	−130
1atn	ΔG_{el}	−45796	−43720	−40084	−36851	−34123	−31514	−29228	−27330
	$\Delta\Delta G_{el}$	−53	−48	−59	−73	−103	−144	−181	−213
1avx	ΔG_{el}	−23678	−22504	−20272	−18115	−16272	−14552	−13066	−11846
	$\Delta\Delta G_{el}$	−474	−473	−487	−497	−529	−566	−613	−657
1b6c	ΔG_{el}	−27210	−26020	−23682	−21188	−18952	−16858	−15001	−13440
	$\Delta\Delta G_{el}$	20	21	23	26	33	38	50	65
1beb	ΔG_{el}	−32291	−31412	−29810	−28156	−26631	−25147	−23792	−22603
	$\Delta\Delta G_{el}$	−32	−20	−28	−57	−71	−91	−107	−117
1brs	ΔG_{el}	−11592	−11121	−10126	−9055	−8060	−7082	−6209	−5491
	$\Delta\Delta G_{el}$	−9	4	−4	−38	−69	−96	−121	−143
1buh	ΔG_{el}	−23443	−22389	−20309	−18157	−16226	−14363	−12722	−11367
	$\Delta\Delta G_{el}$	−4	−3	0	10	30	40	61	73
1h1v	ΔG_{el}	−53147	−50968	−46929	−43069	−39649	−36404	−33593	−31214
	$\Delta\Delta G_{el}$	65	76	78	92	94	114	146	197
1he8	ΔG_{el}	−61945	−59048	−53460	−47992	−43215	−38849	−35058	−31823
	$\Delta\Delta G_{el}$	12	11	7	9	27	14	−5	−5
1kxp	ΔG_{el}	−61074	−59078	−55212	−51137	−47334	−43605	−40331	−37577
	$\Delta\Delta G_{el}$	10	13	9	−7	4	24	24	9
1sbb	ΔG_{el}	−31396	−29839	−26757	−23646	−20853	−18146	−15783	−13853
	$\Delta\Delta G_{el}$	40	43	50	56	80	110	135	161
1ysl	ΔG_{el}	−69136	−67038	−63300	−59813	−56728	−53866	−51382	−49291
	$\Delta\Delta G_{el}$	−21	−3	7	12	35	7	−38	−78
2hp0	ΔG_{el}	−48480	−46080	−41773	−37751	−34226	−30989	−28172	−25779
	$\Delta\Delta G_{el}$	119	139	173	201	202	156	103	45
2uy1	ΔG_{el}	−59581	−57517	−53323	−48714	−44448	−40334	−36703	−33576
	$\Delta\Delta G_{el}$	−158	−146	−159	−177	−220	−267	−328	−368

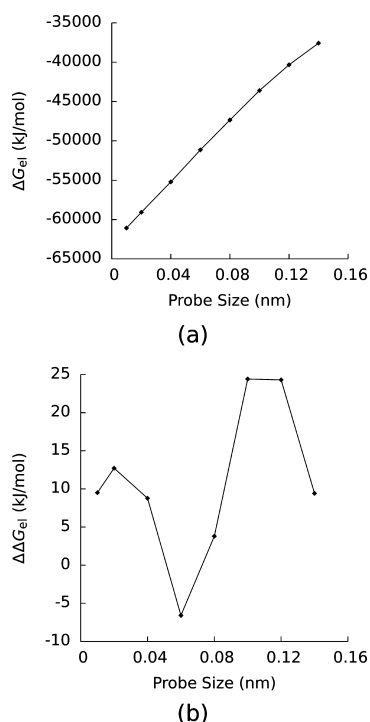[a]Both ΔG_{el} and $\Delta\Delta G_{el}$ are in units of kJ/mol.

Figure 8. Electrostatic (a) solvation and (b) binding free energies (ΔG_{el} and $\Delta\Delta G_{el}$) of one of the complexes in this study (pdbid: 1kxp) as functions of the probe radius used to define the modified van der Waals surface.

potentially revolutionizing drug development and discovery. Unfortunately, PB methods have been less successful at predicting $\Delta\Delta G$ than ΔG.[23−30]

At first glance, the idea that PB methods could be successful at predicting ΔG but fail to predict $\Delta\Delta G$ seems self-contradictory. As shown in eq 1, $\Delta\Delta G_{el}$ can be computed by combining estimates of ΔG_{el} with estimates of $\Delta\Delta G_{el}^{C}$. Part of the reason for this seeming contradiction may be that $\Delta\Delta G_{el}$, as in the present study, is sometimes orders of magnitude smaller than ΔG_{el}, and therefore estimates of ΔG_{el} that have reasonably small relative errors can lead to estimates of $\Delta\Delta G_{el}$ with large relative errors. In the present study ΔG_{el} covered a range of tens of thousands of kJ/mol, whereas $\Delta\Delta G_{el}$ only covered a range of hundreds of kJ/mol. Rankings of these molecules by ΔG_{el} were almost independent of surface definition and choice of force field, whereas rankings of these complexes by $\Delta\Delta G_{el}$ were very sensitive to these details.

One reason that $\Delta\Delta G_{el}$ is difficult to compute may be its sensitivity to the choice of force field. Modern force fields, such as the AMBER[31] and CHARMM[32] force fields, use approximate classical energy functions to model the underlying quantum mechanical interactions, and whether these methods can accurately predict $\Delta\Delta G$, even when the degrees of freedom of the solvent are included, is unclear. The results presented here are consistent with those of other studies that show that current force fields are accurate enough to accurately rank small molecules by ΔG.[3−5] Additionally, the rankings of these complexes by $\Delta\Delta G_{el}$ were not much affected by changing the force field, but although the rankings of the complexes examined here did not change significantly when different force fields were used, the absolute differences in $\Delta\Delta G_{el}$ were large enough that they could cause problems for applications where the differences in $\Delta\Delta G_{el}$ between different complexes were smaller.

Another potential source of uncertainties in $\Delta\Delta G_{el}$ is the uncertainty in how the interface between the interior and exterior of the molecule should be defined. Many different surface definitions have been created (e.g., the SE surface,[36,37] the vdW surface,[38−40] Gaussian surfaces,[41,42] and self-consistent surfaces[43−47]), and no clear consensus has emerged on which of these surface definitions is most realistic. In the present study both the SE and vdW surfaces produced consistent rankings of these molecules by ΔG_{el}, although the absolute differences in ΔG_{el} between these two surface definitions could be quite large. In contrast, the estimates of $\Delta\Delta G_{el}$ produced by these two surface definitions were not correlated. ($R^2 = 0.16$ for the AMBER force field, and 0.17 for CHARMM.) Even the mvdW surface, which was designed to mimic the SE surface, produced estimates of $\Delta\Delta G_{el}$ that were uncorrelated with those given by the SE surface. ($R^2 = 0.13$ for the AMBER force field and 0.30 for CHARMM.) Until the question of how to define the molecular surface is more settled, the PBE will not be able to produce estimates of $\Delta\Delta G_{el}$ accurate enough to be useful for the systems considered here. Of course, only a small number of complexes were considered here and the PBE may be more reliable for other systems, but the data shown here indicate that the sensitivity of $\Delta\Delta G_{el}$ to the exact method that is used to define the molecular surface may help explain why PBE methods have not been uniformly successful at predicting $\Delta\Delta G$.

In conclusion, explaining why PB methods have been fairly successful at predicting ΔG but have been much less successful at predicting $\Delta\Delta G$ appears to be difficult at first glance because $\Delta\Delta G_{el}$ can be computed by combining estimates of ΔG_{el} with $\Delta\Delta G_{el}^{C}$. However, ΔG_{el} is typically orders of magnitude larger than $\Delta\Delta G_{el}$, and therefore estimates of ΔG_{el} must be very accurate if they are to combine to give accurate estimates of $\Delta\Delta G_{el}$. For these reasons, studies that compare the predictions of ΔG by PB methods to experimental results will probably not be sufficient for improving the predictions of $\Delta\Delta G$ given by these methods because the ability of a particular model to predict consistent estimates of ΔG_{el} does not guarantee that it will produce consistent estimates of $\Delta\Delta G_{el}$.

■ AUTHOR INFORMATION

Corresponding Author
*Phone: 850 6447961. Fax: 850 6447244. E-mail: mfenley@sb.fsu.edu.

Notes
The authors declare no competing financial interest.

■ ACKNOWLEDGMENTS

■ REFERENCES

(1) Allen, M. P.; Tildesley, D. J. *Computer Simulation of Liquids*; Oxford University Press: New York, 1987.

(2) Frenkel, D.; Smit, B. *Understanding Molecular Simulation From Algorithms to Applications*; Academic Press: San Diego, 2002.

(3) Guthrie, J. P. A Blind Challenge for Computational Solvation Free Energies: Introduction and Overview. *J. Phys. Chem. B* **2009**, *113*, 4501−4507.

(4) Mobley, D. L.; Bayly, C. I.; Cooper, M. D.; Shirts, M. R.; Dill, K. A. Small Molecule Hydration Free Energies in Explicit Solvent: An

Extensive Test of Fixed-Charge Atomistic Simulations. *J. Chem. Theory Comput.* **2009**, *5*, 350−358.

(5) Mobley, D. L.; Wymer, K. L.; Lim, N. M.; Guthrie, J. P. Blind Prediction of Solvation Free Energies From the SAMPL4 Challenge. *J. Comput.-Aided Mol. Des.* **2014**, *28*, 135−150.

(6) Grochowski, P.; Trylska, J. Continuum Molecular Electrostatics, Salt Effects, and Counterion Binding—A Review of the Poisson-Boltzmann Theory and its Modifications. *Biopolymers* **2008**, *89*, 93−113.

(7) Bardhan, J. P. Biomolecular Electrostatics—I Want Your Solvation (Model). *Comput. Sci. Discovery* **2012**, *5*, 013001.

(8) Li, C.; Li, L.; Petukh, M.; Alexov, E. Progress in Developing Poisson−Boltzmann Equation Solvers. *Mol. Based Math. Biol.* **2013**, *1*, 42−62.

(9) Botello-Smith, W. M.; Cai, Q.; Luo, R. Biological Applications of Classical Electrostatics Methods. *J. Theor. Comput. Chem.* **2014**, *13*, 1440008.

(10) Xiao, L.; Wang, C.; Luo, R. Recent Progress in Adapting Poisson−Boltzmann Methods to Molecular Simulations. *J. Theor. Comput. Chem.* **2014**, *13*, 1430001.

(11) Jean-Charles, A.; Nicholls, A.; Sharp, K.; Honig, B.; Tempczyk, A.; Hendrickson, T. F.; Still, W. C. Electrostatic Contributions to Solvation Energies: Comparison of Free Energy Perturbation and Continuum Calculations. *J. Am. Chem. Soc.* **1991**, *113*, 1454−1455.

(12) Mohan, V.; Davis, M. E.; McCammon, J. A.; Pettitt, B. M. Continuum Model Calculations of Solvation Free Energies: Accurate Evaluation of Electrostatic Contributions. *J. Phys. Chem.* **1992**, *96*, 6428−6431.

(13) Simonson, T.; Bruenger, A. T. Solvation Free Energies Estimated from Macroscopic Continuum Theory: An Accuracy Assessment. *J. Phys. Chem.* **1994**, *98*, 4683−4694.

(14) Dejaegere, A.; Karplus, M. Analysis of Coupling Schemes in Free Energy Simulations: A Unified Description of Nonbonded Contributions to Solvation Free Energies. *J. Phys. Chem.* **1996**, *100*, 11148−11164.

(15) Nicholls, A.; Mobley, D. L.; Guthrie, J. P.; Chodera, J. D.; Bayly, C. I.; Cooper, M. D.; Pande, V. S. Predicting Small-Molecule Solvation Free Energies: An Informal Blind Test for Computational Chemistry. *J. Med. Chem.* **2008**, *51*, 769−779.

(16) Misra, V. K.; Hecht, J. L.; Sharp, K. A.; Friedman, R. A.; Honig, B. Salt Effects on Protein-DNA Interactions: The *λ*cI Repressor and EcoRI Endonuclease. *J. Mol. Biol.* **1994**, *238*, 264−280.

(17) Misra, V. K.; Honig, B. On the Magnitude of the Electrostatic Contribution to Ligand-DNA Interactions. *Proc. Natl. Acad. Sci. U. S. A.* **1995**, *92*, 4691−4695.

(18) Bredenberg, J.; Boschitsch, A. H.; Fenley, M. O. The role of anionic protein residues on the salt dependence of the binding of aminoacyl-tRNA synthetases to tRNA: a Poisson-Boltzmann analysis. *Commun. Comput. Phys.* **2008**, *3*, 1051−1070.

(19) Bredenberg, J. H.; Russo, C.; Fenley, M. O. Salt-mediated electrostatics in the association of TATA binding proteins to DNA: a combined molecular mechanics/Poisson-Boltzmann study. *Biophys. J.* **2008**, *94*, 4634−4645.

(20) Fenley, M. O.; Harris, R. C.; Jayaram, B.; Boschitsch, A. H. Revisiting the Association of Cationic Groove-Binding Drugs to DNA Using a Poisson-Boltzmann Approach. *Biophys. J.* **2010**, *99*, 879−886.

(21) Fenley, M. O.; Russo, C.; Manning, G. S. Theoretical assessment of the oligolysine model for ionic interactions in protein−DNA complexes. *J. Phys. Chem. B* **2011**, *115*, 9864−9872.

(22) Harris, R. C.; Bredenberg, J. H.; Silalahi, A. R. J.; Boschitsch, A. H.; Fenley, M. O. Understanding the physical basis of the salt dependence of the electrostatic binding free energy of mutated charged ligand−nucleic acid complexes. *Biophys. Chem.* **2011**, *156*, 79−87.

(23) Wang, J.; Morin, P.; Wang, W.; Kollman, P. A. Use of MM-PBSA in Reproducing the Binding Free Energies to HIV-1 RT of TIBO Derivatives and Predicting the Binding Mode to HIV-1 RT of Efavirenz by Docking and MM-PBSA. *J. Am. Chem. Soc.* **2001**, *123*, 5221−5230.

(24) Brown, S. P.; Muchmore, S. W. High-Throughput Calculation of Protein−Ligand Binding Affinities: Modification and Adaptation of the MM-PBSA Protocol to Enterprise Grid Computing. *J. Chem. Inf. Model.* **2006**, *46*, 999−1005.

(25) Hou, T.; Wang, J.; Li, Y.; Wang, W. Assessing the Performance of the MM/PBSA and MM/GBSA Methods. 1. The Accuracy of Binding Free Energy Calculations Based on Molecular Dynamics Simulations. *J. Chem. Inf. Model.* **2011**, *51*, 69−82.

(26) Adler, M.; Beroza, P. Improved Ligand Binding Energies Derived from Molecular Dynamics: Replicate Sampling Enhances the Search of Conformational Space. *J. Chem. Inf. Model.* **2013**, *53*, 2065−2072.

(27) Harris, R. C.; Mackoy, T.; Fenley, M. O. A Stochastic Solver of the Generalized Born Model. *Mol. Based Math. Biol.* **2013**, *1*, 63−74.

(28) Li, M.; Petukh, M.; Alexov, E.; Panchenko, A. R. Predicting the Impact of Missense Mutations on Protein−Protein Binding Affinity. *J. Chem. Theory Comput.* **2014**, *10*, 1770−1780.

(29) Muddana, H. S.; Fenley, A. T.; Mobley, D. L.; Gilson, M. K. The SAMPL4 Host−Guest Blind Prediction Challenge: An Overview. *J. Comput.-Aided Mol. Des.* **2014**, 1−13.

(30) Zhu, Y.-L.; Beroza, P.; Artis, D. R. Including Explicit Water Molecules as Part of the Protein Structure in MM/PBSA Calculations. *J. Chem. Inf. Model.* **2014**, *54*, 462−469.

(31) Cornell, W. D.; Cieplak, P.; Bayly, C. I.; Gould, I. R.; Merz, K. M.; Ferguson, D. M.; Spellmeyer, D. C.; Fox, T.; Caldwell, J. W.; Kollman, P. A. A Second Generation Force Field for the Simulation of Proteins, Nucleic Acids, and Organic Molecules. *J. Am. Chem. Soc.* **1995**, *117*, 5179−5197.

(32) MacKerell, A. D., Jr.; et al. All-atom empirical potential for molecular modeling and dynamics studies of proteins. *J. Phys. Chem. B* **1998**, *102*, 3586−3616.

(33) Sitkoff, D.; Ben-Tal, N.; Honig, B. Calculation of Alkane to Water Solvation Free Energies Using Continuum Solvent Models. *J. Phys. Chem.* **1996**, *100*, 2744−2752.

(34) Nina, M.; Beglov, D.; Roux, B. Atomic Radii for Continuum Electrostatics Calculations Based on Molecular Dynamics Free Energy Simulations. *J. Phys. Chem. B* **1997**, *101*, 5239−5248.

(35) Green, D. F. Optimized Parameters for Continuum Solvation Calculations with Carbohydrates. *J. Phys. Chem. B* **2008**, *112*, 5238−5249.

(36) Alexov, E. Role of the Protein Side-Chain Fluctuations on the Strength of Pair-Wise Electrostatic Interactions: Comparing Experimental with Computed pKas. *Proteins: Struct., Funct., Bioinf.* **2003**, *50*, 94−103.

(37) Connolly, M. L. Solvent-Accessible Surfaces of Proteins and Nucleic Acids. *Science* **1983**, *221*, 709−713.

(38) Dong, F.; Vijayakumar, M.; Zhou, H.-X. Comparison of Calculation and Experiment Implicates Significant Electrostatic Contributions to the Binding Stability of Barnase and Barstar. *Biophys. J.* **2003**, *85*, 49−60.

(39) Dong, F.; Zhou, H.-X. Electrostatic Contribution to the Binding Stability of Protein-Protein Complexes. *Proteins: Struct., Funct., Bioinf.* **2006**, *65*, 87−102.

(40) Alsallaq, R.; Zhou, H.-X. Electrostatic Rate Enhancement and Transient Complex of Protein-Protein Association. *Proteins: Struct., Funct., Bioinf.* **2008**, *71*, 320−335.

(41) Friedrichs, M.; Zhou, R.; Edinger, S. R.; Friesner, R. A. Poisson-Boltzmann Analytical Gradients for Molecular Modeling Calculations. *J. Phys. Chem. B* **1999**, *103*, 3057−3061.

(42) Grant, J. A.; Pickup, B. T.; Nicholls, A. A Smooth Permittivity Function for Poisson-Boltzmann Solvation Methods. *J. Comput. Chem.* **2001**, *22*, 608−640.

(43) Dzubiella, J.; Swanson, J. M. J.; McCammon, J. A. Coupling Nonpolar and Polar Solvation Free Energies in Implicit Solvent Models. *J. Chem. Phys.* **2006**, *124*, 084905.

(44) Cheng, L.-T.; Dzubiella, J.; McCammon, J. A.; Li, B. Application of the Level-Set Method to the Implicit Solvation of Nonpolar Molecules. *J. Chem. Phys.* **2007**, *127*, 084503.

(45) Cheng, L.-T.; Wang, Z.; Setny, P.; Dzubiella, J.; Li, B.; McCammon, J. A. Interfaces and Hydrophobic Interactions in Receptor-Ligand Systems: A Level-Set Variational Implicit Solvent Approach. *J. Chem. Phys.* **2009**, *131*, 144102.

(46) Chen, Z.; Baker, N. A.; Wei, G. W. Differential Geometry Based Solvation Model I: Eulerian Formulation. *J. Comput. Phys.* **2010**, *229*, 8231−8258.

(47) Chen, Z.; Baker, N. A.; Wei, G. W. Differential Geometry Based Solvation Model II: Lagrangian Formulation. *J. Math. Biol.* **2011**, *63*, 1139−1200.

(48) Lu, Q.; Luo, R. A Poisson-Boltzmann dynamics method with nonperiodic boundary condition. *J. Chem. Phys.* **2003**, *119*, 11035−11047.

(49) Hu, C. Y.; Kokubo, H.; Lynch, G. C.; Bolen, D. W.; Pettitt, B. M. Backbone additivity in the transfer model of protein solvation. *Protein Sci.* **2010**, *19*, 1011−1022.

(50) Kokubo, H.; Hu, C. Y.; Pettitt, B. M. Peptide Conformational Preferences in Osmolyte Solutions: Transfer Free Energies of Decaalanine. *J. Am. Chem. Soc.* **2011**, *133*, 1849−1858.

(51) Kokubo, H.; Harris, R. C.; Asthagiri, D.; Pettitt, B. M. Solvation Free Energies of Alanine Peptides: The Effect of Flexibility. *J. Phys. Chem. B* **2013**, *117*, 16428−16435.

(52) Harris, R. C.; Pettitt, B. M. Effects of geometry and chemistry on hydrophobic solvation. *Proc. Natl. Acad. Sci. U. S. A.* **2014**, *111*, 14681−14686.

(53) Berman, H. M.; Westbrook, J.; Feng, Z.; Gilliland, G.; Bhat, T. N.; Weissig, H.; Shindyalov, I. N.; Bourne, P. E. The Protein Data Bank. *Nucleic Acids Res.* **2000**, *28*, 235−242.

(54) Dolinsky, T. J.; Nielsen, J. E.; McCammon, J. A.; Baker, N. A. PDB2PQR: An Automated Pipeline for the Setup of Poisson-Boltzmann Electrostatics Calculations. *Nucleic Acids Res.* **2004**, *32*, W665−W667.

(55) Dolinsky, T. J.; Czodrowski, P.; Li, H.; Nielsen, J. E.; Jensen, J. H.; Klebe, G.; Baker, N. A. PDB2PQR: Expanding and Upgrading Automated Preparation of Biomolecular Structures for Molecular Simulations. *Nucleic Acids Res.* **2007**, *35*, W522−W525.

(56) Boschitsch, A. H.; Fenley, M. O. A fast and robust Poisson-Boltzmann solver based on adaptive Cartesian grids. *J. Chem. Theory Comput.* **2011**, *7*, 1524−1540.

(57) Boschitsch, A. H.; Fenley, M. O. A New Outer Boundary Formulation and Energy Corrections for the Nonlinear Poisson−Boltzmann Equation. *J. Comput. Chem.* **2007**, *28*, 909−921.

(58) Harris, R. C.; Boschitsch, A. H.; Fenley, M. O. Influence of Grid Spacing in Poisson-Boltzmann Equation Binding Energy Estimation. *J. Chem. Theory Comput.* **2013**, *9*, 3677−3685.

(59) Cooper, C. D.; Bardhan, J. P.; Barba, L. A. A Biomolecular Electrostatics Solver Using Python, GPUs and Boundary Elements that can Handle Solvent-Filled Cavities and Stern Layers. *Comput. Phys. Commun.* **2014**, *185*, 720−729.